Light-Induced High-Spin Signals from the Oxygen Evolving Center in Ca^{2+}-Depleted Photosystem II Studied by Dual Mode Electron Paramagnetic Resonance Spectroscopy†

Hiroyuki Mino,*,‡ Asako Kawamori,§ Takaya Matsukawa,§ and Taka-aki Ono‡

Photosynthesis Research Laboratory, The Institute of Physical and Chemical Research (RIKEN), Wako, Saitama 351-0198, Japan, and Faculty of Science, Kwansei Gakuin University, Nishinomiya 662-8501, Japan

Received October 6, 1997; Revised Manuscript Received January 7, 1998

ABSTRACT: Illuminating Ca^{2+}-depleted photosystem (PS) II membranes generated two new EPR signals at $g = 11$ and 15 by perpendicular and parallel polarization modes, respectively. Two turnovers of the oxygen evolving center (OEC) beyond the modified S_2' state are required for the appearance of these signals. The formation of the signals correlated with that of an asymmetric (singlet-like) EPR signal observed at $g \approx 2$. Spectral simulation indicated that both signals arose from a transition between $|2^{\pm}>$ levels with intradoublet splitting of $\Delta = 0.276$ cm^{-1} in an $S = 2$ spin system. Furthermore, the two signals in parallel and perpendicular modes were formed at the same time, indicating that the same metal center was responsible. The molecular *z*-axis of the $S = 2$ spin system for the signals was almost parallel to the plane of thylakoid membranes. These results indicate that the Mn cluster in the photosynthetic oxygen evolving center is the source of the new EPR species which may be a Mn(IV)−Mn(IV) or Mn(III)−Mn(III) dimer or a Mn(III) monomer. Redox events of the Mn cluster in the Ca^{2+}-depleted PS II are discussed based on these observations.

Photosynthetic oxygen evolution is carried out by an oxygen evolving center (OEC) containing a tetranuclear Mn cluster located at the lumenal side of photosystem (PS) II protein complexes. Oxidized equivalents generated in the PS II reaction center by the successive absorption of four photons accumulate on the Mn cluster and are used for water oxidation. Molecular oxygen is produced by reactions with five distinct kinetically characterized, intermediate states labeled S_i ($i = 0-4$), of which S_1 is thermally stable in the dark. By absorbing each photon, the S_1 state advances stepwise to reach the highest oxidation state, S_4, that decays spontaneously to the S_0 state with the concurrent release of molecular oxygen (reviewed in refs 1−4). The S-state transitions are accompanied by cyclic changes in the oxidation state of the Mn cluster (*5, 6*), although the valences of manganese ions in the respective S states remain a matter of debate.

Calcium is an indispensable metal cofactor for the normal function of an OEC. Oxygen evolution is inhibited by Ca^{2+} depletion and is restored by reconstitution of Ca^{2+}. It has been proposed that Ca^{2+} is associated with the Mn cluster presumably through a carboxylate bridge (*7*) and that Ca^{2+} depletion directly affects the electronic structure of the Mn cluster (*8*). The S_2 state formed in Ca^{2+}-depleted PS II is abnormally stable. It is manifested as a modified multiline EPR signal with a greater overall width and number of lines, as well as reduced hyperfine splitting, as compared with the normal multiline signal in untreated control PS II (*9*−*12*).

Upon illuminating the Ca^{2+}-depleted PS II in the S_2 state, another EPR signal with a 13−16 mT splitting line width appears around $g = 2$ (*13*). This signal has been called the "S_3-state signal", although it has not been clearly correlated with the normal S_3 state because the latter does not generate EPR signal in the oxygen evolving PS II. "S_3-state signal" has been observed in Cl^--depleted, NH_4Cl-treated and acetate-treated PS II (*14*−*18*), although the *g* value and line width of the signals varied with the preparation.

The "S_3-state signal" has been thought to originate from an organic radical with $S = 1/2$ interacting with the S_2-state Mn cluster, where an oxidized histidine has been ascribed to the radical on the basis of UV−visible and FTIR spectra (*19, 20*). Alternatively, it has been proposed that $Y_Z^{\bullet}$ is attributable to the radical species responsible for the "S_3-state signal" (*15*). In fact, pulsed ENDOR[1] and ESEEM spectra for the "S_3-state signal" were similar to those of a tyrosine radical (*21*−*23*).

Recently, Astashkin et al. (*24*) reported that the "S_3-state signal" involves two signals that overlap at the $g \approx 2$ region. Short illumination of the Ca^{2+}-depleted PS II at 273 K in the S_2 state results in the formation of a doublet signal with splitting of about 15 mT at $g \approx 2$. Further illumination at 273 K led to the formation of a singlet-like signal. Adding DCMU after formation of the stable S_2 state did not inhibit generation of the doublet signal but inhibited that of the singlet-like signal, indicating that at least two turnovers

† This work was supported by Grant-in-Aid for Special Postdoctoral Researchers Program (to H.M.) from RIKEN, by Scientific Research from the Ministry of Education, Science and Culture of Japan (No. 09235237 and No. 09640783) (to T.O.), and by Hyogo Science and Technical Association Foundation (to A.K.). T.O. is indebted to a special Grant for Promotion of Research from RIKEN.

* To whom correspondence should be addressed.

‡ RIKEN.

§ Kwansei Gakuin University.

[1] Abbreviations: MES, 2-morpholinoethanesulfonic acid; MOPS, 4-morpholinopropanesulfonic acid; DCMU, 3-(3,4-dichlorophenyl)-1,1-dimethylurea; ENDOR, electron nuclear double resonance; ESEEM, electron spin-echo envelope modulation.

S0006-2960(97)02471-9 CCC: $15.00
Published on Web 02/13/1998

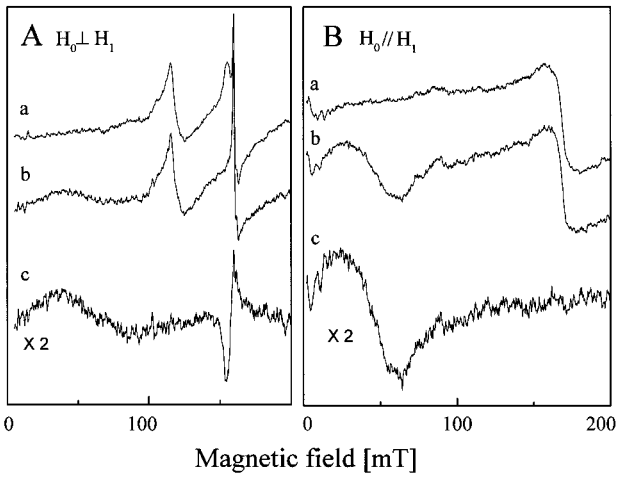

FIGURE 1: EPR spectra detected in Ca^{2+}-depleted PS II membranes by perpendicular (A) and parallel polarization (B) modes: spectra of dark-adapted membranes (a), after illumination for 1 min at 273 K (b), and light-minus-dark difference spectra (c). EPR conditions for perpendicular mode: microwave frequency, 9.684 GHz; microwave power, 0.2 mW; field modulation amplitude, 8 G at 100 kHz; scan time, 168 s; time constant, 0.2 s; temperature, 6 K. EPR conditions for the parallel mode: microwave frequency, 9.345 GHz; microwave power, 3.2 mW; field modulation amplitude, 8 G at 100 kHz; scan time, 168 s; time constant, 0.2 s; temperature, 6 K.

beyond the S_2 state are required for formation of the latter signal. Pulsed ENDOR-induced EPR indicates that $Y_Z^{\bullet}$ is associated with the doublet signal, but not with the singlet-like signal. Therefore, the redox events in the Ca^{2+}-depleted OEC are more complex than was previously considered.

In this paper, we describe a new EPR species that is generated after illumination of the Ca^{2+}-depleted PS II for 20−30 s at 273 K. This species produced EPR signals at low magnetic fields ($g = 11-15$) in parallel polarized and in conventional (perpendicular) modes. The signals showed non-Kramers behavior and were attributed to an $S = 2$ spin system. These and other observations suggest that the signals originate from a monomeric Mn(III), a Mn(IV)−Mn(IV) dimer, or a Mn(III)−Mn(III) dimer.

MATERIALS AND METHODS

Oxygen evolving PS II membranes were prepared from spinach as described (*25*) with modifications (*26*). The membranes were washed twice with a solution containing 400 mM sucrose, 20 mM NaCl, and 0.1 mM MES/NaOH (pH 6.5) and resuspended in the same buffer solution. For Ca^{2+} depletion, the membranes were suspended in a medium containing 400 mM sucrose, 20 mM NaCl, and 10 mM citric acid/NaOH (pH 3.0) at 273 K for 5 min, and then 10% volume of a solution containing 400 mM sucrose, 20 mM NaCl, and 500 mM MOPS/NaOH (pH 7.5) was added to adjust the final pH to about 6.5, as described (*27*). The treated membranes were washed and resuspended in a final buffer solution containing 400 mM sucrose, 20 mM NaCl, and 20 mM MES/NaOH (pH 6.5). All procedures were carried out in the dark or under a dim green light to maintain the OEC in the S_1 state unless otherwise noted. Some of the Ca^{2+}-depleted membrane samples (0.5 mg of Chl/mL) were illuminated for 1 min followed by dark adaptation for 30 min to bring the OEC into the dark-stable S_2 state. DCMU (0.05 mM, 10 mM dimethyl sulfoxide solution as stock) was then added to the solution to ensure a single electron-transfer event beyond the S_2 state.

Membrane samples were collected by centrifugation at 35000*g* for 20 min and transferred to Suprasil quartz tubes of 4-mm inner diameter. The final chlorophyll concentration was approximately 20 mg of Chl/mL. To measure angular dependence of the EPR spectra, membrane samples suspended in a buffer solution containing 400 mM sucrose, 20 mM NaCl, 0.5 mM EDTA, and 20 mM MES/NaOH (pH 6.5) were dried on pieces of Mylar sheets for 12 h at 4 °C under wet N_2 stream; 6−8 pieces of Mylar sheets were put into an EPR tube. The EPR tubes were sealed after Ar gas purge and then stored in liquid N_2 until use. EPR samples were illuminated with a 500-W tungsten−halogen lamp through a 8-cm thick water filter at 273 K.

Conventional (perpendicular) and parallel polarization mode EPR measurements were performed using a Bruker ESP 300E X-band spectrometer and a ER4116 DM X-band (TE_{102}) dual mode resonator. The microwave frequency was changed to resonate in perpendicular and parallel modes. An Oxford 900 continuous-flow cryostat was used to regulate the sample temperature at 6 K.

RESULTS

Figure 1 shows the effect of illumination for 60 s at 273 K on perpendicular EPR (A) and parallel polarized EPR (B) spectra in Ca^{2+}-depleted PS II membranes. The light (trace b) minus dark (trace a) difference spectrum (trace c) reveals a broad signal at approximate magnetic field of 50 mT with a peak-to-peak width of about 40−50 mT in perpendicular or parallel mode measurement. The *g* values of the perpendicular and parallel mode signals were 11 and 15, where resonating microwave frequencies were 9.68 and 9.34 GHz, respectively. The S_1-state Mn cluster in untreated PS II shows a broad signal at approximately 150 mT ($g = 4.9$) with a line width of about 60 mT detected by parallel mode (*28*). However, Figure 1B shows no indication of the S_1-state signal which is consistent with the report that S_1 signals are undetectable in Ca^{2+}-depleted PS II (*28*). These signals observed at $g = 11$ and 15 were not detected in Mn-depleted sample washed by Tris buffer (data not shown). The relatively high background in the spectrum (panel B, traces a and b) was due to impurities in the sample tubes. A derivative type sharp signal detected by perpendicular mode at approximately 150 mT in the difference spectrum (panel A, trace c) was ascribed to artifacts of signal subtraction due to the presence of a sharp signal of rhombic iron and partly to an anomalous signal that appeared in the region, although its intensity varied among samples. It is of note that the anomalous signal was not detected by the parallel mode detection as shown in Figure 1B.

Figure 2A shows illumination for 60 s at 273 K induced the so-called "S_3-state signal" at $g = 2$ in Ca^{2+}-depleted PS II membranes (trace a). This signal disappeared after dark adaptation concomitant with the formation of the modified multiline signal (Figure 2A, trace b) and then was regenerated by further illumination of the dark-adapted membranes (Figure 2A, trace c) in agreement with the reported results (*9*−*12*). Figure 2B (perpendicular detection) and 2C (parallel detection) shows that both new signals disappeared after dark adaptation (trace b) and were regenerated by further illumination (trace c). The reversible formation of the new signals implies that they are not due to PS II damaged by prolonged illumination. The results showed that the forma-

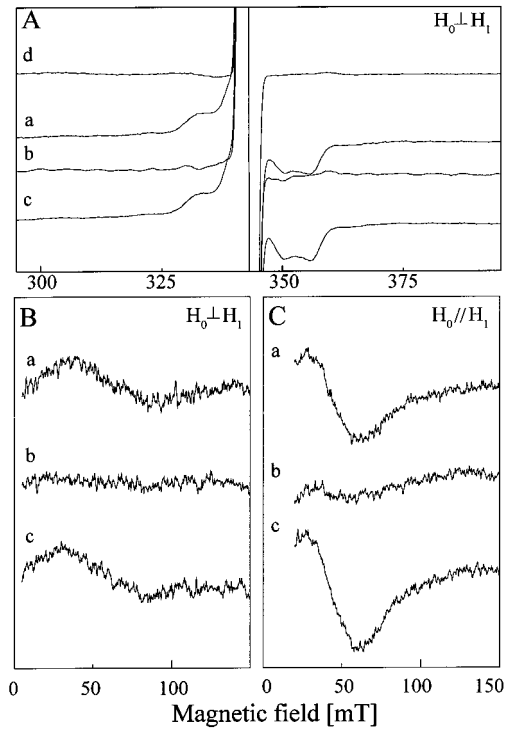

FIGURE 2: Effects of illumination on perpendicular (A, B) and parallel (C) mode EPR spectra in Ca^{2+}-depleted PS II membranes. EPR spectra (B, C) were obtained after subtraction of the dark-adapted spectrum. PS II membranes were dark-adapted (d in panel A), illuminated for 1 min at 273 K (a), dark-adapted again for 60 min at 273 K after illumination (b), and illuminated again for 1 min at 273 K (c). EPR conditions were the same as those described in the legend to Figure 1.

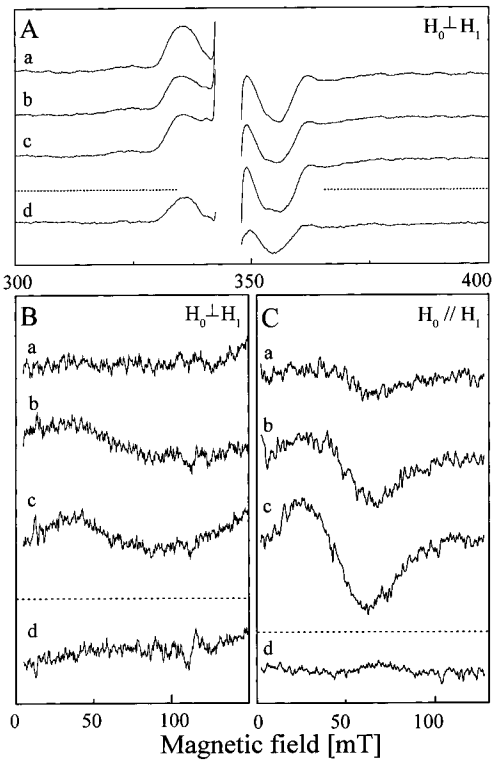

FIGURE 3: Effects of illumination time and addition of DCMU on perpendicular (A, B) and parallel (C) mode EPR. PS II membranes were sequentially illuminated for 1 min at 273 K, dark-adapted for 60 min at 273 K, and then illuminated for 5 s (a), 20 s (b), and 60 s (c, d) at 273 K. DCMU (50 μM) was added to the membrane samples before the second illumination for trace d. Spectra are shown after subtracting S_1 spectrum of dark-adapted membranes (a−c) or S_2 spectrum of the membranes dark-adapted for the second time after illumination (d). EPR conditions are the same as those described in the legend to Figure 1. See text for details.

tion of both new signals clearly correlates with that of the "S_3-state signal".

Figure 3 shows light minus dark difference EPR spectra detected by perpendicular (panels A and B) and parallel (panel C) modes in Ca^{2+}-depleted PS II. The membranes were illuminated for 60 s followed by dark adaptation for 1 h to accumulate the dark-stable S_2-state and then illuminated at 273 K for (trace a) 5 s, (trace b) 20 s, and (trace c) 60 s. The perpendicular (panel B) and parallel (panel C) mode signals developed almost simultaneously during illumination and reached the steady-state high level after illumination for 60 s. As shown in Figure 3A, the shape of the "S_3-state signal" also changed depending on the length of illumination time. Illumination for 5 s produced a 16 mT wide, symmetrical doublet signal. However, the shape of the signal significantly changed, becoming rather asymmetric upon further illumination (>20−30 s), and no further change was induced after illumination for 60 s. Similar spectral change of the so-called "S_3-state signal" has been reported, when the Ca^{2+}-depleted PS II was illuminated with varying numbers of repetitive flashes (*29*).

A recent pulsed EPR study has revealed that illuminating Ca^{2+}-depleted PS II induces two different radical species that generate two signals overlapping at $g = 2$ region (*24*). One radical induced by 5-s illumination at 273 K gives the doublet signal with a split of about 15 mT. The other is induced by longer (>20-s) illumination at 273 K to give the singlet-like signal. Therefore, it is conceivable that the illumination-time-dependent change in the $g = 2$ spectrum shown in Figure 3A reflects the cumulative formation of the doublet and singlet-like radical species. The coincident time courses of the formation of these signals suggest that the parallel and perpendicular mode signals associate with the singlet-like species but not with the doublet species.

It has been reported that the doublet and singlet-like signals are generated after one and at least two turnovers of PS II beyond the modified S_2 state (*24*). Adding DCMU to the sample after the formation of the modified S_2 state inhibits the illumination-time-dependent change in the spectrum of the "S_3-state signal" (Figure 3A, trace d), supporting the view that the formation of the singlet-like signal is responsible for the observed change in the $g = 2$ spectrum. DCMU inhibited the formation of both parallel and perpendicular mode signals (trace d in Figure 3B,C). The results strongly indicate that the two new signals correlate with the "singlet-like signal" and that at least two turnovers beyond the S_2 state are required for their formation.

Figure 4 shows the angular dependence of the $g = 15$ parallel polarized EPR signal in the oriented membranes. The signal intensity shows a large anisotropy: the intensity is maximal and minimal at angles of 90° and 0°, respectively, between the external magnetic field direction and the membrane normal. Detection of the species by parallel mode EPR and the large anisotropy of the signal indicate that an $S = 2$ system is responsible for the signal, and the transition between $|2^+>$ and $|2^->$ levels attributes the signal to be represented by eq 4 given in the Appendix.

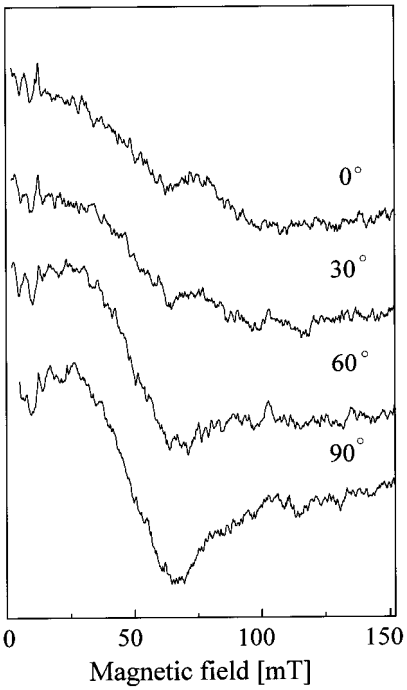

FIGURE 4: Orientation dependence of a low-field EPR signal measured by parallel polarization mode. Ca^{2+}-depleted PS II membranes were illuminated for 1 min at 273 K. Spectra are shown after subtracting S_1 spectrum of the dark-adapted membranes. Numbers represent angle between external magnetic field and the membrane normal. EPR conditions are as described in the legend to Figure 1.

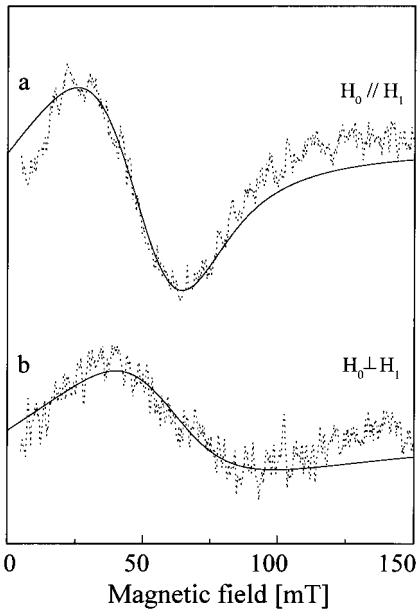

FIGURE 5: Simulation of low-field EPR signals. Light-minus-dark difference spectra with parallel (a) and perpendicular polarization (b) EPR (dotted line) and their simulations (solid line). Ca^{2+}-depleted PS II membranes were illuminated for 1 min at 273 K. Parameters used for simulation were $\Delta = 0.276$ cm^{-1}, $g = 2$, and Gaussian line width = 1000 MHz. EPR signals were detected at 9.35 and 9.68 GHz for parallel and perpendicular mode EPR, respectively, and used for simulation.

The parallel mode signal was then simulated by diagonalizing $S = 2$ spin Hamiltonians (eqs 1 and 2) for every magnetic field value. The transition probability was evaluated by calculating $<2^+|S_z'|2^->$ for the signal. A g value of 2 was assumed since the simulation is not sensitive to a relatively small change in the g anisotropy. The results of the simulation are shown in Figure 5a (solid line) with the experimentally obtained signal (dotted line). The signal was simulated by assuming an intradoublet splitting parameter of $\Delta = 0.276$ cm^{-1}. Notably, the perpendicular mode signal can be simulated (trace b in Figure 5) with the same intradoublet splitting parameter that was determined by simulation of the parallel mode signal, where the transition probability was evaluated by $<2^+|S_x'|2^->$. The result indicates that the two signals originate from the transition between $|2^+>$ and $|2^->$ levels in the $S = 2$ state of a single magnetic center, although the possibility that two magnetic centers with identical magnetic moments are responsible for the two signals cannot be completely excluded. The Δ value obtained by the spectral simulation coincided with that independently deduced from the g values and the resonated microwave frequency of the perpendicular ($g = 15$ at 9.35 GHz) and parallel ($g = 11$ at 9.65 GHz) signals using eq 5 (Appendix).

DISCUSSION

The present study demonstrated that illumination of the Ca^{2+}-depleted PS II induces new EPR signals with g values of 15 at 9.35 GHz in parallel mode and of 11 at 9.68 GHz in perpendicular mode. The two signals developed with the same time course and required at least two turnovers of PS II beyond the stable multiline S_2 state. Furthermore, both signals were simulated by assuming an $S = 2$ system using the same intradoublet splitting value, which accounts for the difference in the effective g value of the two signals measured at different microwave frequencies. Therefore, these findings indicate that one magnetic center with a typical $S = 2$ spin system is responsible for generating the two signals at low magnetic field in perpendicular and parallel mode EPR. In this system, a transition between the intradoublet $|2^\pm>$ with $\Delta m_s = 0$ participates in the parallel mode EPR signal and that with $\Delta m_s = \pm 1$ participates in the perpendicular mode. The line shape and field positions of the parallel and perpendicular mode signals found in the study are similar to those reported in $S = 2$ spin system (*30*, *31*).

An $S = 1$ spin system may reveal a signal at low magnetic field, but it does not usually show large anisotropy in the parallel mode (*32*). A half-integer spin system ($S > 3/2$) may also give a low magnetic field signal if D is close to $h\upsilon$. However, the observed signals could not be simulated by assuming S = 3/2, 5/2, and 7/2 (data not shown). In principle, any integer spin systems ($S \geq 3$) can generate a low-field signal that may be indistinguishable from that of the $S = 2$ system, and the possibility that a spin system of $S \geq 3$ contributes to the new EPR signals cannot be completely excluded. However, it is notable that a low-field EPR signal from an $S \geq 3$ system has never been described in the literature as far as the authors know.

The effective g factor of the low-field signals is large, indicating that the signals originate from a transition-metal center (*33*). In PS II membranes, manganese in OEC, and iron in cytochrome b_{559}, the non-heme center, the Rieske iron-sulfur center, and the cytochrome *b*/*f* complex are the transition metals that potentially give the low-field signals. However, signals attributed to the Rieske center ($g \approx 1.9$), high-spin iron in the cytochrome *b*/*f* ($g \approx 3.5$), the cyto-

Scheme 1: Redox Events in OEC Caused by Illuminating Ca^{2+}-Depleted PS II[a]

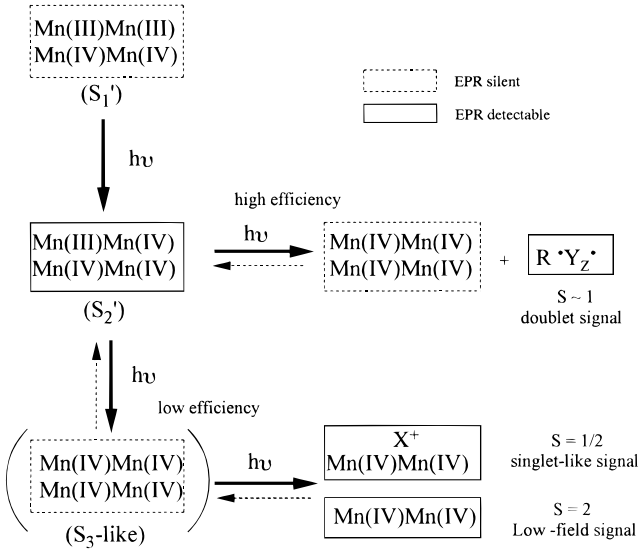

[a] See text for details.

chrome b_{559} ligated by OH^- ($g \approx 5-7$), and the non-heme iron ($g \approx 5-8$) were not induced by illumination for low-field signals as shown in Figures 1 and 3 (*34*−*36*). Some oxidized high-potential cytochrome b_{559} signal was induced by this illumination (data not shown), but oxidation of Fe^{2+} to Fe^{3+} cannot cause the formation of $g = 11-15$ signal that might arise from Fe^{2+} species. Furthermore, the reversible formation of the low-field signals shown in Figure 2 and the time course of the signal generation in Figure 3 are not compatible with the redox reactions of any of the iron centers in PS II. Illumination of the Ca^{2+}-depleted PS II for a short period in the absence of DCMU (Figure 3a−c) generated the doublet signal but did not induce the low-field signals. Therefore the acceptor side of PS II is not associated with the low-field signals.

We conclude from these considerations that the only transition metal attributable to the $S = 2$ spin system in PS II is manganese. $S = 2$ state EPR spectra similar to the low-field signals found in this study have been reported in synthetic Mn(III) monomer and μ_2-carboxo-μ_2-oxo-bridged Mn(III)−Mn(III) dimer (*37*). Therefore, a monomeric Mn(III) nuclei, dimeric Mn(III)−Mn(III), or dimeric Mn(IV)−Mn(IV) is a good candidate for generating the low-field signals. XAFS and EPR studies have demonstrated one or two di-μ_2-oxo-bridged Mn dimers in the Mn cluster in the OEC (reviewed in refs 1−4). The low-field signals, however, cannot be ascribed to the di-μ_2-oxo-bridged Mn dimer, which is strongly antiferromagnetic (*38*), since the exchange interaction for Mn dimers with $S = 2$ spin system in this work may be rather weak.

Astashkin et al. (*24*) have reported that the so-called "S_3-state signal" observed at approximately $g = 2$ consists of doublet and singlet-like signals. The appearance of the doublet signal is accompanied by a 40% decrease in intensity of the stable S_2 multiline signal, probably due to oxidation of the Mn cluster (*21, 24*). It has been suggested that the doublet signal arises from an organic radical pair consisting of $Y_Z^\bullet$ and another one that remains undefined. Although the origin of the singlet-like signal has not been identified, the asymmetric and broad line shape of the signal typical of systems containing a metal center indicates that the singlet-like signal is attributable to the manganese cluster. This is consistent with the loss of the remaining 60% multiline, concomitant with the appearance of the singlet-like signal.

The conditions for the generation and time course of the development of the low-field signals coincided well with those of the singlet-like signal. This indicates that the low-field signals and the singlet-like signal arise from the same PS II center. An $S = 2$ spin system may have a resonance condition at $g = 2$ region in principle, when D is relatively small, but the huge anisotropy of the system broadens the putative signal to become undetectable (*30, 33*). In addition it has been suggested that the singlet-like signal behaves like an $S = 1/2$ spin system (*24*). These imply that the two signals originate from different magnetic centers in the same PS II unit. Since monomeric or dimeric manganese can be responsible for the low-field signals as already discussed, we assume that the Mn cluster is modified by a partial breakage of exchange coupling in the cluster to form a magnetically isolated center responsible for the low-field signals. This may be consistent with the view that a strongly coupled manganese tetramer cannot be attributable to both the $S = 2$ and $S = 1/2$ spin systems.

On the basis of these considerations, we propose a working hypothesis for the reaction scheme of the Mn cluster caused by illumination in the Ca^{2+}-depleted OEC as shown in Scheme 1. The oxidation state of the normal S_2-state Mn cluster is assumed to be Mn(III) + 3Mn(IV) by XANES (*39*). [A study of EPR simulation assumed 3Mn(III) + Mn(IV) (*40*).] The oxidation state of the S_2'-state Mn cluster in Ca^{2+}-depleted sample can be assumed to be Mn(III) + 3Mn(IV) since addition of Ca^{2+} to the membranes in the S_2' state restores the S_2 state exhibiting the normal multiline signal (*1*−*4*). Illumination oxidizes approximately 40% of the S_2-state OEC by 1 equiv to give the radical pair for the doublet signal and the EPR silent 4Mn(IV) cluster (*24*). The remaining 60% of the center is oxidized by 2 equiv to yield the two isolated magnetic centers via an EPR silent state; one is the Mn(IV)−Mn(IV) dimer with an $S = 2$ spin system, and the other is an $S = 1/2$ spin system. We tentatively assume the Mn(IV)−Mn(IV) dimer interacts with a radical (denoted as X^+ in Scheme 1) to give the singlet-like $S = 1/2$ spin state. The quantum efficiency is assumed to be much higher in the doublet signal formation than in the singlet-like and low-field signal formation that involves a structural modification of the Mn cluster. It is of note that the putative structural change will not be due to damage of the OEC caused by prolonged illumination. This is because the dark adaptation led to regeneration of the modified S_2 multiline, concomitant with the disappearance of the low-field and singlet-like signals as shown in Figure 2. Further studies are required to evaluate this scheme and its relationship to the normal S-state cycle.

APPENDIX

The spin Hamiltonians for a spin $S \geq 1$ system in the molecular principal axis frame are given by the following equations (*30, 33*):

$$H_{\text{Zeeman}} = \beta \mathbf{H} \cdot \mathbf{g} \cdot \mathbf{S} \quad (1)$$

$$H_{\text{zero-field}} = D[S_z^2 - {}^1/_3 S(S+1)] + E(S_x^2 - S_y^2) \quad (2)$$

where D and E are rhombic zero-field parameters, β is the Bohr magneton and **g**, the g-tensor.

In an $S = 2$ spin system, the zero-field eigenstates are separated by two non-Kramers doublets, $|2^{s',a}>$ and $|1^{s,a}>$, and a singlet, $|0'>$. The energy levels and eigenstates in zero magnetic field are expressed as

$$E_{2s'} = 2(D^2 + 3E^2)^{1/2},$$

$$|2^{s'}> = \frac{a^+}{\sqrt{2}}(|+2> + |-2>) + a^-|0> \quad (3a)$$

$$E_{2a} = 2D, \qquad |2^{a}> = \frac{1}{\sqrt{2}}(|+2> - |-2>) \quad (3b)$$

$$E_{1s} = -D + 3E, \qquad |1^{s}> = \frac{1}{\sqrt{2}}(|+1> + |-1>) \quad (3c)$$

$$E_{1a} = -D - 3E, \qquad |1^{a}> = \frac{1}{\sqrt{2}}(|+1> - |-1>) \quad (3d)$$

$$E_{0'} = -2(D^2 + 3E^2)^{1/2},$$

$$|0'> = \frac{a^-}{\sqrt{2}}(|+2> + |-2>) - a^+|0> \quad (3e)$$

where

$$a^{\pm} \text{ is } \left(\frac{1}{2}\left[1 \pm \frac{D}{(D^2 + 3E^2)^{1/2}}\right]\right)^{1/2}$$

The eigenfunctions for the EPR detectable transition, within the $|2^{\pm}>$ doublet, are given by the expression:

$$|2^{\pm}> = \alpha^+|2^{s'}> \pm \alpha^-|2^{a}> \quad (4)$$

where $\alpha^{\pm}$ is

$$\left(\frac{1}{2}\left\{1 \pm \frac{\Delta}{[\Delta^2 + (g'\beta H)^2]^{1/2}}\right\}\right)^{1/2}$$

g' is $4g_z a^+ \cos\theta$, g_z is the z-component of g factor, Δ is the energy separation within the doublet ($E_{2s'} - E_{2a}$) defined as $\Delta = 2\,[(D^2 + 3E^2)^{1/2} - D]$, and θ is the angle between the z-axis and $\boldsymbol{H}$ direction. Therefore, the resonance condition is given by

$$(h\upsilon)^2 = \Delta^2 + (g'\beta H_z)^2 \quad (5)$$

REFERENCES

1. Rutherford, A. W., Zimmermann, J.-L., and Boussac, A. (1992) In *The Photosystems: Structure, Function and Molecular Biology* (Barber, J., Ed.) pp 179−229, Elsevier, Amsterdam.
2. Debus, R. J. (1992) *Biochim. Biophys. Acta 1102*, 269−352
3. Sauer, K., Yachandra, V. K., Britt, R. D., and Klein, M. P. (1992) In *Manganese Redox Enzymes* (Pecoraro, V. L., Ed.) pp 105−118, VCH, New York.
4. Britt, R. D. (1996) In *Oxygen Photosynthesis: The Light Reactions* (Ort, D. R., and Yocum, C. F., Ed.) pp 137−164, Kluwer Academic Publisher, Dordrecht.
5. Ono, T., Noguchi, T., Inoue, Y., Kusunoki, M., Matsushita, T., and Oyanagi, H. (1992) *Science 258*, 1335−1337.
6. Roelofs, T. A., Liang, W., Latimer, M. J., Cinco, R. M., Rompel, A., Andrews, J. C., Sauer, K., Yachandra, V. K., and Klein, M. P. (1996) *Proc. Natl. Acad. Sci. U.S.A. 93*, 3335−3340.
7. Noguchi, T., Ono, T., and Inoue, Y. (1995) *Biochim. Biophys. Acta 1228*, 189−200.
8. Ono, T., Noguchi, T., Inoue, Y., Kusunoki, M., Yamaguchi, H., and Oyanagi, H. (1993) *FEBS Lett. 330*, 28−30.
9. Sivaraja, M., Tso, J., and Dismukes, G. C. (1989) *Biochemistry 28*, 9459−9464.
10. Tso, J., Sivaraja, M., Philo, J. S., and Dismukes, G. C. (1991) *Biochemistry 30*, 4740−4747.
11. Ono, T., and Inoue, Y. (1990) *Biochim. Biophys. Acta 1015*, 373−377.
12. Boussac, A., and Rutherford, A. W. (1988) *Biochemistry 27*, 3476−3483.
13. Boussac, A., Zimmermann, J -L., and Rutherford, A. W. (1989) *Biochemistry 28*, 8984−8989.
14. Baumgarten, M., Philo, J. S., and Dismukes, G. C. (1990) *Biochemistry 29*, 10814−10822.
15. Hallahan, B. J., Nugent, H. A., Warden, J. T., and Evans, M. C. W. (1992) *Biochemistry 31*, 4562−4573.
16. MacLachlan, D. J., and Nugent, J. H. A. (1993) *Biochemistry 32*, 9772−9780.
17. MacLachlan, D. J., Nugent, J. H. A., Warden, J. T., and Evans, M. C. W. (1994) *Biochim. Biophys. Acta 1188*, 325−334.
18. Szalai, V. A., and Brudvig, G. W. (1996) *Biochemistry 35*, 1946−1953.
19. Boussac, A., Zimmermann, J.-L., Rutherford, A. W., and Lavergne, J. (1990) *Nature 347*, 303−306.
20. Berthomieu, C., and Boussac, A. (1995) *Biochemistry 34*, 1541−1548
21. Gilchrist, M. L., Ball, J. A., Randall, D. W., and Britt, R. D. (1995) *Proc. Natl. Acad. Sci. U.S.A. 92*, 9545−9549.
22. Tang, X.-S., Randall, D. W., Force, D. A., Diner, B. A., and Britt, R. D. (1996) *J. Am. Chem. Soc. 118*, 7638−7639.
23. Force, D. A., Randall, D. W., and Britt, R. D. (1997) *Biochemistry 36*, 12062−12070.
24. Astashkin, A. V., Mino, H., Kawamori, A., and Ono, T. (1997) *Chem. Phys. Lett. 272*, 506−516.
25. Berthold, D. A., Babcock, G. T., and Yocum, C. F. (1981) *FEBS Lett. 134*, 231−234.
26. Ono, T., and Inoue, Y. (1986) *Biochim. Biophys. Acta 850*, 380−389.
27. Ono, T., and Inoue, Y. (1989) *Biochim. Biophys. Acta 973*, 443−449.
28. Yamauchi, T., Mino, H., Matsukawa, T., Kawamori, A., and Ono, T. (1997) *Biochemistry 36*, 7520−7526.
29. Boussac, A., Rutherford, A. W. (1995) *Biochim. Biophys. Acta 1230*, 195−201.
30. Hendrich, M. P., and Debrunner, P. G. (1989) *Biophys. J.* 489−506.
31. Hargen, W. R. (1982) *Biochim. Biophys. Acta 708*, 82−98.
32. Carrington, A., and McLachlan, A. D. (1967) *Introduction to Magnetic Resonance*, Chapter 8, Harper and Row, New York.
33. Abragam, A., and Bleaney, B. (1970) *Electron Paramagnetic resonance of Transition Ions*, Clarendon Press, Oxford.
34. Miller, A.-F., and Brudvig, G. W. (1991) *Biochim. Biophys. Acta 1056*, 1−18.
35. Fiege, R., Scrieber, U., Renger, G., Lubitz, W., and Shuvalov, V. A. (1995) *FEBS Lett. 377*, 325−329.
36. Hulsebosch, R. J., Hoff, A. J., and Shuvalov, V. A. (1996) *Biochim. Biophys. Acta 1277*, 103−106.
37. Dexheimer, S. L., Gohdes, J. W., Chan, M. K., Hagen, K. S., Armstrong, W. H., and Klein, M. P. (1989) *J. Am. Chem. Soc. 111*, 8923−8925.
38. Wieghardt, B. K. (1989) *Angew. Chem., Int. Ed. Engl. 28*, 1153−1172.
39. Yachandra, V. K., DeRose, V. J., Latimer, M. J., Mukerji, I., Sauer, K., and Klein, M. P. (1993) *Science 260*, 675−679.
40. Zheng, M., and Dismukes, G. C. (1996) *Inorg. Chem. 35*, 3307−3319.

BI972471C